

Naturalness in D-brane Inspired Models

Ron De Benedetti,¹ Tianjun Li,^{2,3} James A. Maxin,¹ and Dimitri V. Nanopoulos^{4,5,6}

¹*Department of Chemistry and Physics, Louisiana State University, Shreveport, Louisiana 71115 USA*

²*CAS Key Laboratory of Theoretical Physics, Institute of Theoretical Physics, Chinese Academy of Sciences, Beijing 100190, P. R. China*

³*School of Physical Sciences, University of Chinese Academy of Sciences, No.19A Yuquan Road, Beijing 100049, P. R. China*

⁴*George P. and Cynthia W. Mitchell Institute for Fundamental Physics and Astronomy, Texas A&M University, College Station, TX 77843, USA*

⁵*Astroparticle Physics Group, Houston Advanced Research Center (HARC), Mitchell Campus, Woodlands, TX 77381, USA*

⁶*Academy of Athens, Division of Natural Sciences, 28 Panepistimiou Avenue, Athens 10679, Greece*

We examine the naturalness of the D-brane inspired model constructed in flipped $SU(5)$ supplemented with vector-like particles at the TeV scale, dubbed flippons. We find the model can produce a mainly Higgsino-like lightest supersymmetric particle (LSP) and small light stops, as favored by naturalness. In fact, a large trilinear scalar A_t term at the electroweak (EW) scale creates a large mass splitting between the top squarks, driving the light stop to near degeneracy with an LSP that is almost all Higgsino, with $\Delta M(\tilde{t}_1, \tilde{\chi}_1^0) < 5$ GeV, evading the LHC constraint on $\tilde{t}_1 \rightarrow c\tilde{\chi}_1^0$ thus far. Given the smallness of the light stop, generating a 125 GeV light Higgs boson mass is aided by one-loop contributions from the Yukawa couplings between the flippons and Higgs fields. The resulting parameter space satisfying naturalness is rather constrained, thus we assess its viability by means of comparison to the LHC constraint on soft charm jets and direction detection limits on spin-independent cross-sections. Finally, we compute the level of electroweak fine-tuning and uncover a region with $\Delta_{EW} < 30$, *i.e.*, fine-tuning better than 3%, regarded as low electroweak fine-tuning. Given the small light stop, the electroweak fine-tuning from only the top squarks is of $\mathcal{O}(1)$, indicating no fine-tuning from neither the light stop \tilde{t}_1 nor the heavy stop \tilde{t}_2 .

PACS numbers: 11.10.Kk, 11.25.Mj, 11.25.-w, 12.60.Jv

INTRODUCTION

The null results at the 13 TeV LHC Run 2 (LHC2) regarding the search for supersymmetry (SUSY) have now extended through 2018, as recent results find only Standard Model (SM) background events for data collected from 2016-18, inclusive of 137 fb^{-1} [1]. The rather strong limits derived from these observations though rely upon gluino (\tilde{g}) and light stop (\tilde{t}_1) channels producing hard jets via $\tilde{g} \rightarrow \tilde{t}_1 t \rightarrow t\tilde{t}\tilde{\chi}_1^0$ and $\tilde{g} \rightarrow q\tilde{q}\tilde{\chi}_1^0$, leading to limits on the gluino mass in excess of 2 TeV and on the light stop mass above 1 TeV. Such hard jets are easily accessible at the LHC2, affirming the rapid uninterrupted march to multi-TeV exclusion limits, yet approaching tension with SUSY's solution to the hierarchy problem, a prime reason motivating SUSY in the first place. On the other hand, the empty SUSY cupboard thus far prompts one to ask as to whether SUSY could be hiding in plain sight?

Natural SUSY, referred to as naturalness, strives for negligible electroweak fine-tuning in SUSY grand unified theory (GUT) models, defined by only natural cancellations amid terms in the tree-level minimization condition on the Higgs potential, plus radiative corrections. Insignificant amounts of fine-tuning require small terms in the minimization condition such that all terms on both sides of the equation are of comparable scale in order to compute the measured Z-boson mass. Such

natural dynamics are very desirable, although an additional benefit can be realized that relates to the dilemma posed in the prior paragraph. The principal contributor to loop-level corrections are top squarks, so naturalness stresses small values for $M(\tilde{t}_1)$, but small light stops could provoke degeneracy in the form of $M(\tilde{t}_1) \sim M(\tilde{\chi}_1^0)$. This raises an element of uncertainty for accessibility at the LHC, given the softness of these light stop events and hence unreliable distinction from the ubiquitous SM background. Indeed, one could expect these soft interactions to evade observation at the LHC if the light stop becomes rather compressed with the LSP. Furthermore, a complication surfaces with insufficient 1-loop and 2-loop SUSY contributions to the light Higgs boson mass m_h from a small light stop, failing to generate the observed $m_h = 125.09 \pm 0.24$ GeV [2, 3] light Higgs boson mass. We now introduce a model that has minimal electroweak fine-tuning but can handily achieve consistency with the light Higgs boson mass constraints, as well as other key experimental measurements, and could be flying just under the SUSY radar.

We shall study the flipped $SU(5)$ model [4–6] in this paper, where the gauge group $SU(5) \times U(1)_X$ can be embedded into the $SO(10)$ model. The flipped $SU(5)$ models can be constructed from the four-dimensional free fermionic string construction [7–9], orbifold [10, 11] and Calabi-Yau [12] compactifications of the heterotic $E_8 \times E_8$ string theory, intersecting D-brane model build-

ing [13–15], as well as F-theory model building [16, 17]. In addition, two of us (TL and DVN) with Jiang proposed the testable flipped $SU(5)$ models where the TeV-scale vector-like multiplets, dubbed flippons, are introduced, and string-scale gauge coupling unification can be achieved [18]. Such kind of models can be constructed from the four-dimensional free fermionic string construction [9], intersecting D-brane model building [15], as well as F-theory model building [16, 17], and was referred to as \mathcal{F} - $SU(5)$. This model persists in two classes: (i) the minimalistic formalism of the one-parameter version implementing vanishing No-Scale SUGRA soft SUSY breaking terms at the unification scale (For example, see Refs. [19–22] and references therein), and (ii) the general formalism with non-universal SUSY soft breaking terms mirroring the flipped $SU(5)$ GUT representation, inspired by D-brane model building, and thus informally designated the \mathcal{F} - $SU(5)$ D-brane inspired model [23]. This second approach endures as merely a D-brane *inspired* model and not a formally constructed D-brane model by reason of forbidden Yukawa coupling terms in the Higgs and Yukawa superpotentials, though we discuss in the next section possible methods to elude these hurdles. The \mathcal{F} - $SU(5)$ D-brane inspired model revealed a possible region of naturalness featuring small light stops and a Higgsino-like lightest supersymmetric particle (LSP) [23], which we shall more fully unpack here in this work. For a discussion of naturalness in a Pati-Salam model constructed from intersecting D6-branes in Type IIA string theory, see Ref. [24].

Fine-tuning in the minimalistic formalism of \mathcal{F} - $SU(5)$ has been explored [25]. In Ref. [25] it was shown that the contemporary measures of fine-tuning we shall employ in this analysis are essentially structurally similar to an original fine-tuning measure, Δ_{EENZ} [26, 27], first prescribed some 30 years ago by Ellis, Enqvist, Nanopoulos, and Zwirner (EENZ). The one-parameter version of the model possesses an intrinsic proportional dependence of all model scales on the unified gaugino mass parameter $M_{1/2}$, inclusive of the Z -boson mass expressed as a simple quadratic function of $M_{1/2}$. The implication was electroweak fine-tuning of unity scale [25]. The minimalistic version of \mathcal{F} - $SU(5)$ is presently under probe at the LHC2 [28] and has thus far survived the 13 TeV LHC2 137 fb^{-1} results [1]. Now we turn our attention to the less internally constrained version of \mathcal{F} - $SU(5)$, evaluating fine-tuning in the D-brane inspired model. Our goal here is to show that this class of \mathcal{F} - $SU(5)$ is inflicted with a minimal amount of fine-tuning also, and even though the one-parameter version is presently experiencing a direct probe by the LHC, the naturalness sector of the D-brane inspired model has been just *under* the reach of the LHC2.

In this work we first supply a brief review of the flipped $SU(5)$ class of models and the D-brane inspired model in particular. Then we delve into the comprehensive numer-

ical procedure necessary to investigate naturalness. Once the numerical approach has been wholly dissected, we expand upon the phenomenology of the naturalness sector and the attainment of small light stops, Higgsino-like LSPs, and other associated provisions essential for low fine-tuning, accompanied by light Higgs boson masses lifted to 125 GeV for many points by the vector-like flippon contributions. Integrated into this analysis will be evidence of our naturalness sector skirting under the LHC constraints up to this point, and moreover, an evaluation against dark matter direct detection experiments and application of their results as a constraint on the naturalness region. Finally, we conclude with the fine-tuning calculations and assessment of the numerical findings.

REVIEW OF \mathcal{F} - $SU(5)$ MODEL

We review here only the primary principles of \mathcal{F} - $SU(5)$. In the minimal flipped $SU(5)$ model [4–6], the gauge group $SU(5) \times U(1)_X$ can be embedded within the $SO(10)$ model. Please see Refs. [20–22, 25, 29] and references therein for a more in-depth analysis of the minimal flipped $SU(5)$ model. The generator $U(1)_{Y'}$ in $SU(5)$ is defined as

$$T_{U(1)_{Y'}} = \text{diag} \left(-\frac{1}{3}, -\frac{1}{3}, -\frac{1}{3}, \frac{1}{2}, \frac{1}{2} \right), \quad (1)$$

and as a result the hypercharge is given by

$$Q_Y = \frac{1}{5} (Q_X - Q_{Y'}). \quad (2)$$

There are three families of the SM fermions with quantum numbers under $SU(5) \times U(1)_X$ given by, respectively,

$$F_i = (\mathbf{10}, \mathbf{1}), \quad \bar{f}_i = (\bar{\mathbf{5}}, -\mathbf{3}), \quad \bar{l}_i = (\mathbf{1}, \mathbf{5}), \quad (3)$$

where $i = 1, 2, 3$. The SM particle assignments in F_i , \bar{f}_i and \bar{l}_i are

$$F_i = (Q_i, D_i^c, N_i^c), \quad \bar{f}_i = (U_i^c, L_i), \quad \bar{l}_i = E_i^c, \quad (4)$$

where Q_i , U_i^c , D_i^c , L_i , E_i^c and N_i^c are the left-handed quark doublets, right-handed up-type quarks, down-type quarks, left-handed lepton doublets, right-handed charged leptons, and neutrinos, respectively. The introduction of three SM singlets ϕ_i can generate the heavy right-handed neutrino masses.

The GUT and electroweak gauge symmetries are broken through the introduction of the two pairs of Higgs representations

$$\begin{aligned} H &= (\mathbf{10}, \mathbf{1}), \quad \bar{H} = (\bar{\mathbf{10}}, -\mathbf{1}), \\ h &= (\mathbf{5}, -\mathbf{2}), \quad \bar{h} = (\bar{\mathbf{5}}, \mathbf{2}). \end{aligned} \quad (5)$$

The H multiplet states are labeled by the same symbols as the F multiplet, and for \bar{H} we only add a “bar” above the fields. Specifically, the Higgs particles are

$$H = (Q_H, D_H^c, N_H^c), \quad \bar{H} = (\bar{Q}_H, \bar{D}_H^c, \bar{N}_H^c), \quad (6)$$

$$h = (D_h, D_h, D_h, H_d), \quad \bar{h} = (\bar{D}_h, \bar{D}_h, \bar{D}_h, H_u), \quad (7)$$

where H_d and H_u are one pair of Higgs doublets in the MSSM.

The ensuing Higgs superpotential at the GUT scale breaks the $SU(5) \times U(1)_X$ gauge symmetry down to the SM gauge symmetry

$$W_{\text{GUT}} = \lambda_1 H H h + \lambda_2 \overline{H H h} + \Phi(\overline{H H} - M_H^2). \quad (8)$$

Merely one F-flat and D-flat direction exists, and that can be rotated along the N_H^c and $\overline{N_H^c}$ directions. Consequently, we have $\langle N_H^c \rangle = \langle \overline{N_H^c} \rangle = M_H$. With the exception of D_H^c and $\overline{D_H^c}$, the superfields H and \overline{H} are “eaten” and acquire substantial masses via the supersymmetric Higgs mechanism. Moreover, the superpotential terms $\lambda_1 H H h$ and $\lambda_2 \overline{H H h}$ couple D_H^c and $\overline{D_H^c}$ respectively with D_h and \overline{D}_h , which forms massive eigenstates with masses $2\lambda_1 \langle N_H^c \rangle$ and $2\lambda_2 \langle \overline{N_H^c} \rangle$. Therefore, the doublet-triplet splitting due to the missing partner mechanism [6] naturally arises. However, the triplets in h and \bar{h} only have a small mixing via the μ term, so the colored Higgsino-exchange mediated proton decay is negligible, *i.e.*, there is no dimension-5 proton decay problem.

The following vector-like particles (flippions) at the TeV scale are introduced to realize string-scale gauge coupling unification [16–18]

$$\begin{aligned} XF &= (\mathbf{10}, \mathbf{1}), \quad \overline{XF} = (\overline{\mathbf{10}}, -\mathbf{1}), \\ Xl &= (\mathbf{1}, -\mathbf{5}), \quad \overline{Xl} = (\mathbf{1}, \mathbf{5}). \end{aligned} \quad (9)$$

The particle content from the decompositions of XF , \overline{XF} , Xl , and \overline{Xl} under the SM gauge symmetry are

$$\begin{aligned} XF &= (XQ, XD^c, XN^c), \quad \overline{XF} = (XQ^c, XD, XN), \\ Xl &= (XE), \quad \overline{Xl} = (XE^c). \end{aligned} \quad (10)$$

The quantum numbers for the extra vector-like particles under the $SU(3)_C \times SU(2)_L \times U(1)_Y$ gauge symmetry are

$$XQ = (\mathbf{3}, \mathbf{2}, \frac{1}{6}), \quad XQ^c = (\overline{\mathbf{3}}, \mathbf{2}, -\frac{1}{6}), \quad (11)$$

$$XD = (\mathbf{3}, \mathbf{1}, -\frac{1}{3}), \quad XD^c = (\overline{\mathbf{3}}, \mathbf{1}, \frac{1}{3}), \quad (12)$$

$$XN = (\mathbf{1}, \mathbf{1}, \mathbf{0}), \quad XN^c = (\mathbf{1}, \mathbf{1}, \mathbf{0}), \quad (13)$$

$$XE = (\mathbf{1}, \mathbf{1}, -\mathbf{1}), \quad XE^c = (\mathbf{1}, \mathbf{1}, \mathbf{1}). \quad (14)$$

The superpotential is

$$\begin{aligned} W_{\text{Yukawa}} &= y_{ij}^D F_i F_j h + y_{ij}^{U\nu} F_i \bar{f}_j \bar{h} + y_{ij}^{E\bar{l}} \bar{l}_i \bar{f}_j h \\ &+ \mu h \bar{h} + y_{ij}^N \phi_i \overline{H} F_j + M_{ij}^\phi \phi_i \phi_j \\ &+ y_{XF} X F X F h + y_{\overline{XF}} \overline{X F X F h} \\ &+ M_{XF} \overline{X F X F} + M_{Xl} \overline{X l X l}, \end{aligned} \quad (15)$$

and the above superpotential after the $SU(5) \times U(1)_X$ gauge symmetry is broken down to the SM gauge symmetry gives

$$\begin{aligned} W_{SSM} &= y_{ij}^D D_i^c Q_j H_d + y_{ij}^{U\nu} U_i^c Q_j H_u + y_{ij}^E E_i^c L_j H_d \\ &+ y_{ij}^{U\nu} N_i^c L_j H_u + \mu H_d H_u + y_{ij}^N \langle \overline{N_H^c} \rangle \phi_i N_j^c \\ &+ y_{XF} X Q X D^c H_d + y_{\overline{XF}} X Q^c X D H_u \\ &+ M_{XF} (X Q^c X Q + X D^c X D) \\ &+ M_{Xl} X E^c X E + M_{ij}^\phi \phi_i \phi_j \\ &+ \dots (\text{decoupled below } M_{GUT}). \end{aligned} \quad (16)$$

where y_{ij}^D , $y_{ij}^{U\nu}$, y_{ij}^E , y_{ij}^N , y_{XF} , and $y_{\overline{XF}}$ are Yukawa couplings, μ is the bilinear Higgs mass term, and M_{ij}^ϕ , M_{XF} and M_{Xl} are masses for new particles. The new particles are the vector-like flippions, though we shall not formally compute the masses M_{ij}^ϕ , M_{XF} , and M_{Xl} in this study, reserving this analysis for the future. Only a common mass decoupling scale M_V for the flippion vector-like particles is enforced. Present LHC constraints on vector-like T and B quarks [30] fix lower limits of about 855 GeV for (XQ, XQ^c) vector-like flippions and 735 GeV for (XD, XD^c) vector-like flippions. We therefore suitably place our lower M_V limit at $M_V \geq 855$ GeV to guarantee inclusion of all experimentally viable flippion masses in our work.

The two-stage unification of flipped $SU(5)$ [4–6] allows for fundamental GUT scale Higgs representations (not adjoints), natural doublet-triplet splitting, suppression of dimension-five proton decay [31], and a two-step see-saw mechanism for neutrino masses [32, 33]. More precisely, a distinct separation between the ultimate $SU(5) \times U(1)_X$ unification at around 3×10^{17} GeV and the penultimate $SU(3)_C \times SU(2)_L$ unification near 10^{16} GeV emerges due to revisions to the one-loop gauge β -function coefficients b_i to include contributions from the vector-like flippion multiplets that induce the required flattening of the $SU(3)$ Renormalization Group Equation (RGE) running ($b_3 = 0$) [19]. The $M2$ and $M3$ gaugino mass terms are unified into a single mass term $M5 = M2 = M3$ [34], and hence $\alpha_5 = \alpha_2 = \alpha_3$, at the $SU(3)_C \times SU(2)_L$ unification near 10^{16} GeV. The $M1$ gaugino mass term runs up to the $SU(5) \times U(1)_X$ unification at $M_{\mathcal{F}}$, by virtue of a small shift due to $U(1)_X$ flux effects [34] between the $SU(3)_C \times SU(2)_L$ unification around 10^{16} GeV and the $SU(5) \times U(1)_X$ unification around 3×10^{17} GeV [19]. This shift motivates that the $M1$ gaugino mass term above the unification around 10^{16} GeV be referred to as M_{1X} . The scale $M_{\mathcal{F}}$ is defined by unification of the couplings $\alpha_5 = \alpha_{1X}$, which boosts unification to near the string scale and Planck mass. The flattening of the $M3$ gaugino mass dynamic evolution down to the electroweak scale generates the mass texture of $M(\hat{t}_1) < M(\hat{g}) < M(\hat{q})$, with the light stop and gluino lighter than all other squarks [21].

The SUSY breaking soft terms at the $M_{\mathcal{F}}$ scale in the

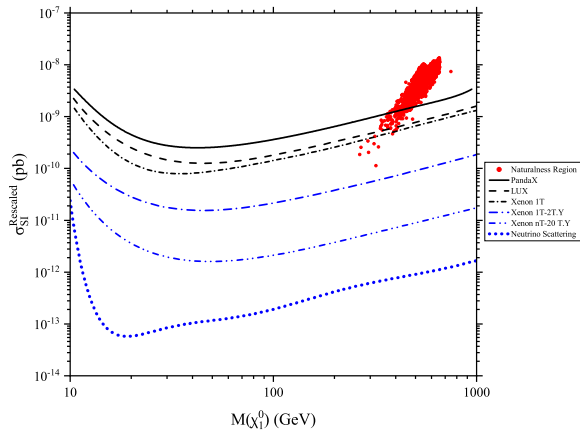


FIG. 1: Depiction of the \mathcal{F} - $SU(5)$ D-brane inspired naturalness region, represented by the small red points. The LUX, PandaX-II, and XENON100 dark matter direct detection upper limits on spin-independent neutralino-nucleus cross-sections are sketched and labeled, as well the neutrino scattering floor. The ~ 2900 points here satisfy the constraints $M(\tilde{g}) \geq 1.6$ TeV, $124 \leq m_h \leq 128$ GeV, $\Omega h^2 \leq 0.1221$, $\Delta M(\tilde{t}_1, \tilde{\chi}_1^0) \leq 10$ GeV, and $\tilde{\chi}_1^0 > 80\%$ Higgsino. The cross-sections $\sigma_{SI}^{\text{Rescaled}}$ are rescaled in accordance with Eq. (17).

\mathcal{F} - $SU(5)$ model are appropriately $M_5, M_{1X}, M_{U^cL}, M_{E^c}, M_{QD^cN^c}, M_{H_u}, M_{H_d}, A_\tau, A_t,$ and A_b . Non-universal SUSY breaking soft terms such as these are inspired partially by D-brane model building [15], where $F_i, \bar{f}_i, \bar{l}_i,$ and h/\bar{h} result from intersections of different stacks of D-branes. In this event, the associated SUSY breaking soft mass terms and trilinear scalar A terms are different, while M_{H_u} is equal to M_{H_d} . Despite the fact the Yukawa terms \overline{HHh} and $\overline{HH\bar{h}}$ of Eq. (8) and $F_i F_j h, X F X F h,$ and $\overline{X F X F \bar{h}}$ of Eq. (15) are forbidden by the anomalous global $U(1)$ symmetry of $U(5)$, these Yukawa terms could be generated from high-dimensional operators or instanton effects. In fact, the $SU(5) \times U(1)_X$ models differ from $SU(5)$ models such that in \mathcal{F} - $SU(5)$ the Yukawa term $F_i F_j h$ gives down-type quark masses, so their Yukawa couplings can be small and be generated via high-dimensional operators or instanton effects.

NUMERICAL APPROACH

At the unification scale of $M_{\mathcal{F}} \sim 3 \times 10^{17}$ GeV, the \mathcal{F} - $SU(5)$ general SUSY breaking soft terms are applied, namely $M_5, M_{1X}, M_{U^cL}, M_{E^c}, M_{QD^cN^c}, M_{H_u} = M_{H_d}, A_\tau, A_t,$ and A_b . The \mathcal{F} - $SU(5)$ unification scale $M_{\mathcal{F}}$ near the string and Planck scale is in contrast to the usual lower GUT scale of about 10^{16} GeV in the MSSM. All SUSY breaking soft terms are allowed to float up to 5 TeV, with the A terms varying between ± 5 TeV,

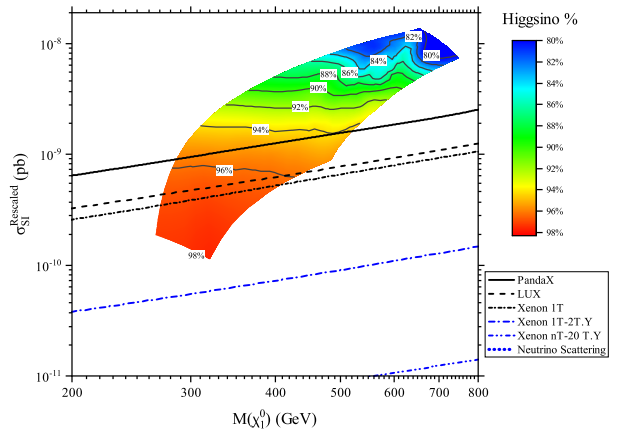


FIG. 2: Smoothly flowing contours of the Higgsino-like LSP percentage within the \mathcal{F} - $SU(5)$ D-brane inspired naturalness region. The LUX, PandaX-II, and XENON100 dark matter direct detection upper limits on spin-independent neutralino-nucleus cross-sections are sketched and labeled. The region illustrated here satisfies the constraints $M(\tilde{g}) \geq 1.6$ TeV, $124 \leq m_h \leq 128$ GeV, $\Omega h^2 \leq 0.1221$, $\Delta M(\tilde{t}_1, \tilde{\chi}_1^0) \leq 10$ GeV, and $\tilde{\chi}_1^0 > 80\%$ Higgsino. The cross-sections $\sigma_{SI}^{\text{Rescaled}}$ are rescaled in accordance with Eq. (17).

though specifically for the A_t term we establish an extended lower limit of -7 TeV. A ± 1.5 GeV margin of error is permitted around the top quark world average of 173.2 GeV [35]. The ratio of the vacuum energy expectation values $\tan\beta$ is allowed to span its entire range of $5 \leq \tan\beta \leq 60$. The flippon vector-like decoupling scale is sampled within the range $855 \leq M_V \leq 23,000$ GeV. We adopt $\mu > 0$ for all points as suggested by the results of $g_\mu - 2$ for the muon.

The model is constrained to be consistent with both the WMAP 9-year [36] and Planck 2018 [37] relic density measurements, imposing an upper limit of $\Omega h^2 \leq 0.1221$. Given the large annihilation cross-section of a Higgsino-like LSP, no lower limit is placed on Ωh^2 . The strongest LHC gluino limits arise from the search regions $\tilde{g} \rightarrow \tilde{q}q \rightarrow q\tilde{q}\tilde{\chi}_1^0$ and $\tilde{g} \rightarrow \tilde{t}_1 t \rightarrow t\tilde{\chi}_1^0$, however, in our study here we are interested in the channel producing a top+charm via $\tilde{g} \rightarrow \tilde{t}_1 t \rightarrow ct\tilde{\chi}_1^0$, which persists with weaker limits. Accordingly, we implement a somewhat weaker lower boundary of $M(\tilde{g}) \geq 1.6$ TeV given that these gluinos are not easily accessible.

The theoretical calculation of the light Higgs boson mass is allowed to vary from the experimental central value of $m_h = 125.09$ GeV, where we account for a 2σ experimental uncertainty and theoretical uncertainty of 1.5 GeV. The allocated range for the flippon Yukawa coupling spans from its minimal value (no coupling between the flippons and Higgs fields) to its maximal value (maximum coupling between flippons and Higgs fields).

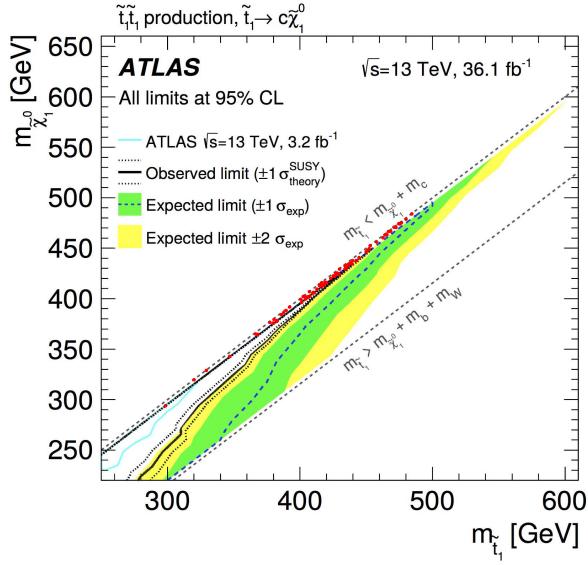


FIG. 3: Layered illustration of the \mathcal{F} - $SU(5)$ D-brane inspired naturalness region (represented by the small red points) superimposed upon the ATLAS Collaboration exclusion curve plot on $\tilde{t}_1\tilde{t}_1$ production in the monojet search region for the channel $\tilde{t}_1 \rightarrow c\tilde{\chi}_1^0$, reprinted from Ref. [39]. The branching fraction for $\tilde{g} \rightarrow \tilde{t}_1 t$ and $\tilde{t}_1 \rightarrow c\tilde{\chi}_1^0$ is nearly 100% for our points shown in this Figure. The naturalness region in this diagram involves the 74 points that satisfy $M(\tilde{g}) \geq 1.6$ TeV, $124 \leq m_h \leq 128$ GeV, $\Omega h^2 \leq 0.1221$, $\sigma_{SI}^{\text{Rescaled}} \leq 1.5 \times 10^{-9}$ pb, and $\Delta M(\tilde{t}_1, \tilde{\chi}_1^0) \leq 5$ GeV. All 74 points depicted here possess an LSP that is at least 92% Higgsino, but no more than 98% Higgsino.

In the maximum case, the light Higgs boson mass calculation consists of the 1-loop and 2-loop SUSY contributions, mainly from the coupling to the light stop, plus the vector-like flippon contributions. This maximal value implies the (XD, XD^c) Yukawa coupling is fixed at $Y_{XD} = 0$ and the (XU, XU^c) Yukawa coupling is set at $Y_{XU} = 1$, while the (XD, XD^c) trilinear coupling A term set at $A_{XD} = 0$ and the (XU, XU^c) A term is fixed at $A_{XU} = A_U = A_0$ [21, 38]. In total, after including all contributions, the light Higgs boson mass calculation must return a value of $124 \leq m_h \leq 128$ GeV.

We further assess the model against rare decay processes, to include the branching ratio of the rare b-quark decay of $Br(b \rightarrow s\gamma) = (3.43 \pm 0.21^{\text{stat}} \pm 0.24^{\text{th}} \pm 0.07^{\text{sys}}) \times 10^{-4}$ [41], the branching ratio of the rare B-meson decay to a dimuon of $Br(B_s^0 \rightarrow \mu^+\mu^-) = (2.9 \pm 0.7 \pm 0.29^{\text{th}}) \times 10^{-9}$ [42], and the 3σ intervals around the Standard Model result and experimental measurement of the SUSY contribution to the anomalous magnetic moment of the muon of $-17.7 \times 10^{-10} \leq \Delta a_\mu \leq 43.8 \times 10^{-10}$ [43]. We only inspect the model versus these

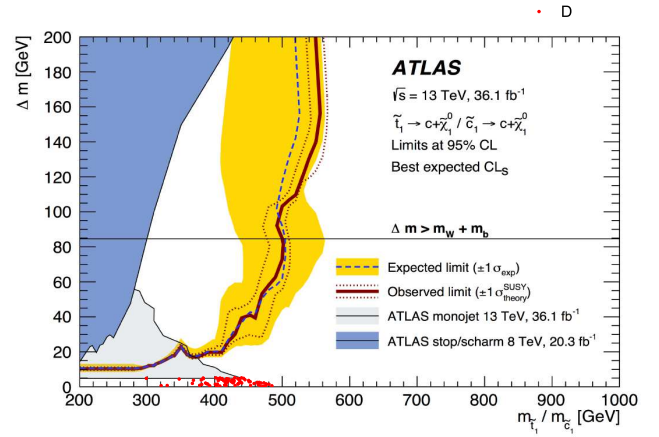


FIG. 4: Layered illustration of the \mathcal{F} - $SU(5)$ D-brane inspired naturalness region (represented by the small red points) superimposed upon the ATLAS exclusion curve plot in the charm jets plus zero lepton (0L) search region for the channel $\tilde{t}_1 \rightarrow c\tilde{\chi}_1^0$, reprinted from Ref. [40]. This ATLAS exclusion plot also includes the monojet search region of Ref. [39]. The branching fraction for $\tilde{g} \rightarrow \tilde{t}_1 t$ and $\tilde{t}_1 \rightarrow c\tilde{\chi}_1^0$ is nearly 100% for our points shown in this Figure. The naturalness region in this diagram involves the 74 points that satisfy $M(\tilde{g}) \geq 1.6$ TeV, $124 \leq m_h \leq 128$ GeV, $\Omega h^2 \leq 0.1221$, $\sigma_{SI}^{\text{Rescaled}} \leq 1.5 \times 10^{-9}$ pb, and $\Delta M(\tilde{t}_1, \tilde{\chi}_1^0) \leq 5$ GeV. All 74 points depicted here possess an LSP that is at least 92% Higgsino, but no more than 98% Higgsino.

rare decay processes, and do not explicitly constrain the model per these experimental limits.

The naturalness region is also evaluated against dark matter direct detection constraints on spin-independent cross-sections σ_{SI} for neutralino-nucleus interactions established by the Large Underground Xenon (LUX) experiment [44], PandaX-II Experiment [45], and XENON100 Collaboration [46]. The relic density calculations involve only the SUSY lightest neutralino $\tilde{\chi}_1^0$ abundance, hence all points must admit alternative components to maintain compatibility with the WMAP 9-year and 2018 Planck total observed relic density, thus the spin-independent cross-section calculations are rescaled as follows:

$$\sigma_{SI}^{\text{Rescaled}} = \sigma_{SI} \frac{\Omega h^2}{0.1200}. \quad (17)$$

The 150 million points scanned in Ref. [23] were enhanced in this effort by an additional 250 million points. The Higgs and SUSY mass spectra, relic density, dark matter direct detection cross-sections, LSP composition, and rare decay processes are calculated with MicrOMEGAs 2.1 [47] employing a proprietary mpi modification of the SuSpect 2.34 [48] codebase to run flippon and general No-Scale \mathcal{F} - $SU(5)$ enhanced RGEs, implementing non-universal soft supersymmetric breaking parameters at the $M_{\mathcal{F}}$ scale. Supersymmetric particle decays are calculated with SUSY-HIT 1.5a [49]. The Particle Data Group [50] world average for the strong cou-

pling constant is $\alpha_S(M_Z) = 0.1181 \pm 0.0011$ at 1σ , and we assume a value in this work of $\alpha_S = 0.1184$.

NATURALNESS PHENOMENOLOGY

Naturalness demands no disproportionate cancellations amongst the terms within the minimization of the Higgs scalar potential with respect to the H_u and H_d directions. The tree-level minimization condition is

$$\frac{M_Z^2}{2} = \frac{M_{H_d}^2 - \tan^2 \beta M_{H_u}^2}{\tan^2 \beta - 1} - \mu^2, \quad (18)$$

however, loop-level radiative corrections to the effective scalar potential $V_{\text{eff}} \rightarrow V_{\text{tree}} + V_{\text{loop}}$ deteriorate the situation further as the quadratic H_u^2 and H_d^2 field coefficients are transformed as $M_{H_u}^2 \rightarrow M_{H_u}^2 + \Sigma_u^u$ and $M_{H_d}^2 \rightarrow M_{H_d}^2 + \Sigma_d^d$. The largest contributions from the radiative corrections Σ_u^u and Σ_d^d emanate from the top squarks \tilde{t}_1 and \tilde{t}_2 , so we will only consider those loop corrections in this study. Provided that we desire no auspicious cancellations on the right-hand side of Eq. (18) in order to produce the correct Z -boson mass, we also require a small bilinear Higgs mixing term μ in addition to the top squarks. Moreover, the quadratic Higgs mass term $M_{H_u}^2$ evolves from a large positive value at the ultimate unification scale $M_{\mathcal{F}}$ to a negative value at the EW scale through RGE running due to the large top quark Yukawa coupling, provoking the need for a small negative $M_{H_u}^2$ as well. In summary, the leading culprits to engender contrived results within Eq. (18) are \tilde{t}_1 , \tilde{t}_2 , μ , and H_u^2 , motivating minimal values for these quantities. We correspondingly seek regions of the D-brane inspired \mathcal{F} - $SU(5)$ parameter space yielding small top squarks, small μ parameter, and a small negative $M_{H_u}^2$ term. A small μ parameter at the EW scale in turn produces light Higgsinos since the Higgsino mass is near μ , and more practically, a dominant Higgsino component of the LSP. Therefore, we further search for regions of the model space with a dominant Higgsino-like LSP.

The initial step involves a search for an LSP that is greater than 80% Higgsino. These points are readily recognized by $M(\tilde{\chi}_2^0) < 0$ on account of the μ term at $M_{\mathcal{F}}$ driven below the gaugino mass terms $M1$ and $M2$ at the electroweak scale via RGE running, sending $\tilde{\chi}_2^0$ to negative values. Another characteristic of spectra with a Higgsino-like LSP is the compressed nature of the $\tilde{\chi}_1^0$, $\tilde{\chi}_1^\pm$, and $\tilde{\chi}_2^0$. The mass deltas expected to produce a Higgsino-like LSP are $\Delta M(\tilde{\chi}_1^\pm, \tilde{\chi}_1^0) \sim 5$ GeV and $\Delta M(\tilde{\chi}_2^0, \tilde{\chi}_1^0) \sim 17$ GeV. Accompanying the Higgsino-like LSP, we further require the condition $\Delta M(\tilde{t}_1, \tilde{\chi}_1^0) \leq 10$ GeV to restrict the results to only those light stops nearly degenerate with the LSP, fulfilling the requisite small light stop limitation. Out of the 400 million points scanned,

the intersection of the experimentally viable constraints on $M(\tilde{g})$, m_h , and Ωh^2 in tandem with an LSP that is $> 80\%$ Higgsino and $\Delta M(\tilde{t}_1, \tilde{\chi}_1^0) \leq 10$ GeV only surrenders ~ 2900 points. The resulting region is illustrated in FIG. 1 and FIG. 2, where the dark matter direct detection upper limits on spin-independent neutralino-nucleus cross-sections are superimposed, along with the neutrino scattering floor. All ~ 2900 points are discretely depicted in FIG. 1, whilst FIG. 2 delineates smoothly flowing contours of this region highlighting Higgsino percentage of the LSP. It is clear in FIG. 2 that the more favorable SUSY spectra in terms of smaller spin-independent cross-sections are the larger Higgsino percentages, exhibiting positive accommodation with both characteristics. All points in FIG. 1 and FIG. 2 have been rescaled in accordance with Eq. (17).

The analysis from this point forward now enforces two more rather strong restrictions. We want to retain only those points possessing $\sigma_{SI}^{\text{Rescaled}} \leq 1.5 \times 10^{-9}$ pb, ensuring consistency with the LUX [44], PandaX-II [45], and XENON100 [46] upper limits illuminated in FIG. 1 and FIG. 2. In the region we are exploring here, $\sigma_{SI}^{\text{Rescaled}} \sim 1.5 \times 10^{-9}$ pb prevails as an approximate upper limit, so we shall now only consider points less than this boundary. We additionally aim to filter out those points inconsistent with LHC model-independent constraints on $\tilde{t}_1 \rightarrow c\tilde{\chi}_1^0$. The nearly degenerate light stop and LSP induce a branching fraction of nearly 100% for $\tilde{g} \rightarrow \tilde{t}_1 t$ and $\tilde{t}_1 \rightarrow c\tilde{\chi}_1^0$. However, given the compression between the light stop and LSP, we expect a rather hard top quark but a very soft charm jet, making extraction of this signal from the SM background challenging to say the least. To assist in comparing our naturalness region to the LHC constraints on $\tilde{t}_1 \rightarrow c\tilde{\chi}_1^0$, post application of $\sigma_{SI}^{\text{Rescaled}} \leq 1.5 \times 10^{-9}$ pb we overlay the remaining points onto the ATLAS Collaboration exclusion curve plot on $\tilde{t}_1 \tilde{t}_1$ production in the monojet search region for the channel $\tilde{t}_1 \rightarrow c\tilde{\chi}_1^0$, reprinted from Ref. [39] and displayed in FIG. 3. In addition, we superimpose our points onto the ATLAS exclusion curve plot in the charm jets plus zero lepton (0L) search region for the channel $\tilde{t}_1 \rightarrow c\tilde{\chi}_1^0$, reprinted from Ref. [40] and shown in FIG. 4. The common element in both these ATLAS Figures is the maximum delta between the light stop and LSP of about 5 GeV, with $\Delta M(\tilde{t}_1, \tilde{\chi}_1^0) \lesssim 5$ GeV persisting as viable due to the soft nature of these events and difficulty in differentiation from the SM background. This theme is uniform between both ATLAS and the CMS Collaboration, as the $\tilde{t}_1 \rightarrow c\tilde{\chi}_1^0$ CMS search regions of Refs. [51–53] paint the same picture of viability for $\Delta M(\tilde{t}_1, \tilde{\chi}_1^0) \lesssim 5$ GeV. The CMS Ref. [54] for pair production of third-generation squarks states that “Top squark masses below 510 GeV are excluded for the scenario in which $\tilde{t}_1 \rightarrow c\tilde{\chi}_1^0$ and the mass splitting between the top squark and the LSP is small”, though Ref. [54] does not explicitly enumerate the value of “small”, hence we shall

TABLE I: The SUSY breaking soft terms, in addition to the vector-like flippon decoupling scale M_V , the low energy ratio of Higgs vacuum expectation values (VEVs) $\tan\beta$, and top quark mass M_t for the \mathcal{F} - $SU(5)$ D-brane inspired naturalness region. Each benchmark point is identified with an alphabetical label in order to link the data in TABLE I with the data in TABLES II - III. All masses are in GeV. The relic density Ωh^2 , rescaled dark matter direct detection cross section $\sigma_{SI}^{\text{Rescaled}}$ (in pb), and Higgsino percentage of the LSP are also given.

Benchmark	M_5	M_{1X}	M_{UcL}	M_{Ec}	M_{QDcNc}	$M_{H_u} = M_{H_d}$	A_τ	A_t	A_b	M_V	$\tan\beta$	M_t	Ωh^2	$\sigma_{SI}^{\text{Rescaled}}$	LSP
A	1500	3200	1300	1300	1700	3400	2750	-2000	-750	17,500	33	173.2	0.0043	8×10^{-10}	95% Higgsino
B	1700	3000	1300	1300	1300	3700	2750	-1900	1000	17,500	29	173.7	0.0060	9×10^{-10}	96% Higgsino
C	1300	4500	1300	2500	1500	3400	-750	-2200	-2500	12,500	29	173.7	0.0015	2×10^{-10}	96% Higgsino
D	1500	3200	1300	1700	1700	3500	4500	-1900	-750	12,500	33	174.2	0.0061	1.5×10^{-9}	94% Higgsino
E	1500	3100	1300	1500	1700	3500	-750	-1900	-2500	12,500	29	174.2	0.0062	1.5×10^{-9}	94% Higgsino
F	1500	3100	1300	1500	1700	3500	2750	-1900	-2500	12,500	29	174.2	0.0045	1.1×10^{-9}	94% Higgsino
G	1500	3200	1700	1300	1700	3600	2750	-2200	-750	20,000	33	174.7	0.0021	2.6×10^{-10}	97% Higgsino
H	1500	3000	1500	1700	1500	3500	-2500	-2000	1000	20,000	33	174.7	0.0038	5.5×10^{-10}	96% Higgsino
I	1500	3100	1500	1300	1700	3500	-750	-2000	-750	17,500	33	174.7	0.0064	1.3×10^{-9}	95% Higgsino

TABLE II: Relevant SUSY spectrum masses for the SUSY breaking soft terms of TABLE I for the \mathcal{F} - $SU(5)$ D-brane inspired naturalness region. The soft SUSY breaking terms that generate each of these spectra can be identified by the alphabetical label. The light Higgs boson mass m_h column represents the theoretically computed value consisting of the 1-loop and 2-loop SUSY contributions *plus* the maximum vector-like flippon contribution. The ΔM columns provide the mass difference between the two SUSY particles given. The $M_{\mathcal{F}}$ value is the unification scale where $\alpha_{1X} = \alpha_5$. All values in this Table are in GeV.

Benchmark	$M(\tilde{\chi}_1^0)$	$M(\tilde{\chi}_2^0)$	$M(\tilde{\chi}_1^\pm)$	$M(\tilde{t}_1)$	$M(\tilde{g})$	$M(\tilde{u}_R)$	m_h	$\Delta M(\tilde{t}_1, \tilde{\chi}_1^0)$	$\Delta M(\tilde{\chi}_1^\pm, \tilde{\chi}_1^0)$	$\Delta M(\tilde{\chi}_2^0, \tilde{\chi}_1^0)$	$A_t(EW)$	$\mu(EW)$	$M_{\mathcal{F}}$
A	388	-406	394	390	2011	3078	124.01	1.3	5.6	17.6	3771	402	3.4×10^{17}
B	425	-442	432	428	2254	3323	124.64	2.7	6.3	16.4	4197	439	3.0×10^{17}
C	294	-310	298	298	1732	2978	125.40	4.6	4.4	16.4	3559	306	3.6×10^{17}
D	420	-440	426	423	1997	3124	124.53	3.1	5.9	19.7	3755	437	3.7×10^{17}
E	415	-435	421	419	1996	3108	124.96	3.6	6.2	19.9	3774	432	3.6×10^{17}
F	416	-436	422	417	1996	3108	124.87	0.5	6.2	20.0	3773	433	3.6×10^{17}
G	329	-344	334	329	2017	3200	125.26	0.5	5.3	15.3	3730	340	3.4×10^{17}
H	343	-359	348	347	2016	3121	124.47	4.2	5.7	16.1	3712	355	3.4×10^{17}
I	406	-425	412	411	2012	3134	124.46	4.5	5.9	18.7	3696	421	3.4×10^{17}

consider $\Delta M(\tilde{t}_1, \tilde{\chi}_1^0) \lesssim 5$ GeV to remain experimentally viable. The administering of $\sigma_{SI}^{\text{Rescaled}} \leq 1.5 \times 10^{-9}$ pb and $\Delta M(\tilde{t}_1, \tilde{\chi}_1^0) \leq 5$ GeV trims the number of residual points from ~ 2900 down to only 74 out of 400 million scan! All 74 points have an LSP composition of at least 92% Higgsino, as FIG. 2 had indicated, though no point is greater than 98% Higgsino, supporting small but non-negligible bino and wino components.

We highlight nine benchmark points in TABLES I - II. All nine benchmarks are amongst the remaining 74 points satisfying all the constraints applied. It should be noted that the light Higgs boson mass m_h in TABLE II includes all SUSY contributions and the vector-like flippon contribution, lifting the Higgs mass for most of the points to their observed value. This is rather beneficial given the smallness of the light stop and hence its diminished loop-level contribution to the Higgs mass. Notice that there is a repetitive pattern to the A_t and $M_{H_u}^2 = M_{H_d}^2$ terms at $M_{\mathcal{F}}$ such that we need $A_t \sim -2000$ GeV and $M_{H_u} = M_{H_d} \sim 3500$ GeV at high scale. This propels consistency within the region for our fine-tuning calculations outlined in the next section.

The entire naturalness model space handily satisfies the B-meson decay and anomalous magnetic moment of

the muon boundaries highlighted in the prior section, with our 74 surviving points falling within $3.2 \times 10^{-9} \leq Br(B_s^0 \rightarrow \mu^+ \mu^-) \leq 3.5 \times 10^{-9}$ and $1.5 \times 10^{-10} \leq \Delta a_\mu \leq 2.9 \times 10^{-10}$. However, with regard to the rare b-quark decay, all remaining 74 points compute to $Br(b \rightarrow s\gamma) \leq 2.34 \times 10^{-4}$, less than the approximate lower 2σ experimental bound of $Br(b \rightarrow s\gamma) \sim 2.77 \times 10^{-4}$, with the smallest of the light stop points returning a value as low as $Br(b \rightarrow s\gamma) \sim 10^{-6}$. This is not surprising, given the smallness of the light stop and chargino. The charged heavy Higgs bosons H^\pm additionally contribute, but not of sufficient magnitude to offset the minimal SUSY contribution from loops regarding stops and charginos. We emphasize that no points have been excluded from this analysis per the inconsistency with experimental limits on the $Br(b \rightarrow s\gamma)$, as we merely note that the SUSY contribution to the total branching ratio is light, thereby suggesting tension with the experimental result.

FINE-TUNING

It was discussed in the prior section that low fine-tuning conforms with small values for $M(\tilde{t}_1)$, $M(\tilde{t}_2)$, μ ,

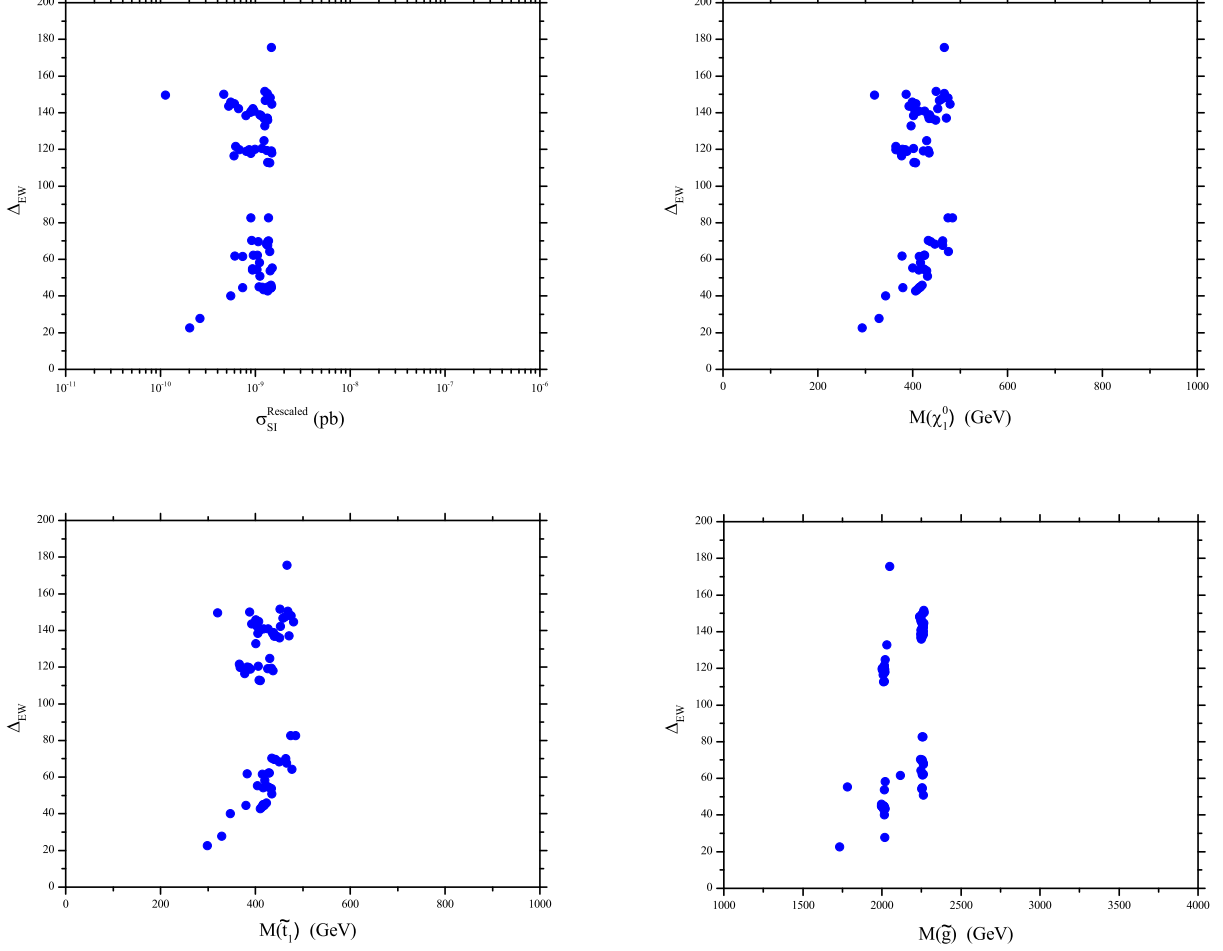


FIG. 5: Electroweak fine-tuning measure Δ_{EW} plot as a function of $\sigma_{SI}^{\text{Rescaled}}$, $M(\tilde{\chi}_1^0)$, $M(\tilde{t}_1)$, and $M(\tilde{g})$ for the \mathcal{F} - $SU(5)$ D-brane inspired naturalness region. The naturalness region in this diagram involves the 74 points that satisfy $M(\tilde{g}) \geq 1.6$ TeV, $124 \leq m_h \leq 128$ GeV, $\Omega h^2 \leq 0.1221$, $\sigma_{SI}^{\text{Rescaled}} \leq 1.5 \times 10^{-9}$ pb, and $\Delta M(\tilde{t}_1, \tilde{\chi}_1^0) \leq 5$ GeV. All 74 points depicted here possess an LSP that is at least 92% Higgsino, but no more than 98% Higgsino. The Δ_{EW} stem exclusively from either $M_{H_u}^2(EW)$ or $\mu^2(EW)$. These plots highlight a region with $\Delta_{EW} < 30$, regarded as low electroweak fine-tuning.

and $M_{H_u}^2$, thus we shall conclude this work with an analytical study of how the naturalness region we uncovered here performs in this realm. We follow the prescription offered in Refs. [55, 56], calculating measures for electroweak scale fine-tuning. Examining each term on the right-hand side of Eq. (18), we have interest in the three electroweak scale tree-level terms

$$C_{H_u} = \left| \frac{-M_{H_u}^2(EW)\tan^2\beta}{\tan^2\beta - 1} \right|, \quad (19)$$

$$C_{H_d} = \left| \frac{M_{H_d}^2(EW)}{\tan^2\beta - 1} \right|, \quad (20)$$

$$C_\mu = |-\mu^2(EW)|, \quad (21)$$

and in the two electroweak scale loop-level terms

$$C_{\tilde{t}_{1,2}} = \left| \frac{3}{16\pi^2} M_{\tilde{t}_{1,2}}^2 \left(\log \frac{M_{\tilde{t}_{1,2}}^2}{Q_{\tilde{t}}^2} - 1 \right) \right. \\ \left. \times \left[Y_t^2 - g_Z^2 \mp \frac{Y_t^2 A_t^2 - 8g_Z^2(\frac{1}{4} - \frac{2}{3}x_w)\Delta_t}{M_{\tilde{t}_2}^2 - M_{\tilde{t}_1}^2} \right] \right|, \quad (22)$$

with $\Delta_t = \frac{1}{2}(M_{\tilde{t}_L}^2 - M_{\tilde{t}_R}^2) + M_Z^2 \cos 2\beta (\frac{1}{4} - \frac{2}{3}x_w)$, $g_Z^2 = \frac{1}{8}(g^2 + g'^2)$, $x_w = \sin^2\theta_W$, $Y_t^2 = Y_t^2(EW)$, and $A_t^2 = A_t^2(EW)$. For the low-energy scale Q , to minimize the

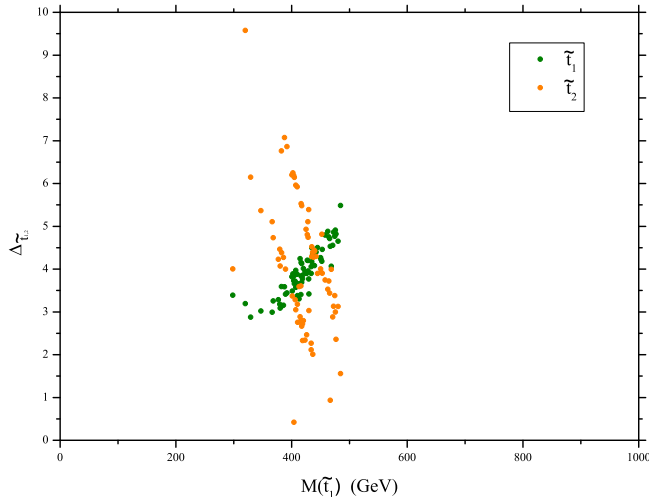


FIG. 6: Electroweak fine-tuning measure $\Delta_{\tilde{t}_{1,2}}$ for only the top squarks \tilde{t}_1 and \tilde{t}_2 , plot as a function of $M(\tilde{t}_1)$ for the \mathcal{F} - $SU(5)$ D-brane inspired naturalness region. The naturalness region in this diagram involves the 74 points that satisfy $M(\tilde{g}) \geq 1.6$ TeV, $124 \leq m_h \leq 128$ GeV, $\Omega h^2 \leq 0.1221$, $\sigma_{SI}^{\text{Rescaled}} \leq 1.5 \times 10^{-9}$ pb, and $\Delta M(\tilde{t}_1, \tilde{\chi}_1^0) \leq 5$ GeV. All 74 points depicted here possess an LSP that is at least 92% Higgsino, but no more than 98% Higgsino. This graph shows that the top squarks contribute very little, if any, fine-tuning to the \mathcal{F} - $SU(5)$ D-brane inspired naturalness region

logarithms in Eq. (22) we use the mean of the top squark masses $Q_{\tilde{t}} = (M_{\tilde{t}_1} + M_{\tilde{t}_2})/2$. The measure of electroweak scale fine-tuning Δ_{EW} adopts the maximum of $C_i = \{C_{H_u}, C_{H_d}, C_\mu, C_{\tilde{t}_1}, C_{\tilde{t}_2}\}$, given by

$$\Delta_{EW} = \frac{\text{Max}(C_i)}{M_Z^2/2}. \quad (23)$$

With our armament of fine-tuning measures in Eqs. (19) - (23) we now proceed to compute Δ_{EW} for the 74 points satisfying all criteria outlined in the prior sections. The results of Δ_{EW} are presented in FIG. 5. We plot them as a function of the primary parameters we are interested in here, namely $\sigma_{SI}^{\text{Rescaled}}$, $M(\tilde{\chi}_1^0)$, $M(\tilde{t}_1)$, and $M(\tilde{g})$. The fine-tuning calculations for the benchmark points are featured in TABLE III, inclusive of the percentage of fine-tuning, simply Δ^{-1} . A diminished amount of fine-tuning is preferred since this indicates that all terms on the right-hand side of Eq. (18), including radiative corrections, are moving contiguous to the scale of the numerical value of the left-hand side. This is represented by a smaller Δ_{EW} in TABLE III and FIG. 5. Equivalently, we can also assess success through the percentage of fine-tuning, where a larger percent is preferred, also itemized in TABLE III. Generally speaking, $\Delta_{EW} < 30$, or coequally fine-tuning better than 3%, is regarded as a low amount of fine-tuning in a SUSY GUT model. The points in FIG. 5 present a region with

$\Delta_{EW} < 30$, with two benchmark points in TABLES I - III possessing this characteristic. While $\Delta_{EW} < 30$ can be viewed as low fine-tuning, our naturalness region also offers several points with $\Delta_{EW} < 50$. Five of these points are amongst our nine benchmark points detailed in TABLES I - III. The maximum EW term for all 74 points emerges from either C_{H_u} or C_μ .

The electroweak fine-tuning from only the top squarks, as represented by Eq. (22), is of $\mathcal{O}(1)$, as expected given the small light stop. If we identify the fine-tuning emanating from only the top squarks as

$$\Delta_{\tilde{t}_{1,2}} = \frac{C_{\tilde{t}_{1,2}}}{M_Z^2/2}, \quad (24)$$

then we see that all 74 of our points possess $\Delta_{\tilde{t}_{1,2}} < 10$, indicating that all of the electroweak fine-tuning arises from either $M_{H_u}^2(EW)$ or $\mu^2(EW)$. This is illustrated in FIG. 6, showing $\Delta_{\tilde{t}_{1,2}}$ versus the light stop mass, with the majority of the points having $\Delta_{\tilde{t}_{1,2}}$ around $\mathcal{O}(1)$. The explicit $\Delta_{\tilde{t}_{1,2}}$ calculations for the nine benchmark points are provided in TABLE III.

TABLE III: Electroweak fine-tuning measures Δ_{EW} and $\Delta_{\tilde{t}_{1,2}}$ for the \mathcal{F} - $SU(5)$ D-brane inspired naturalness region. The fine-tuning percentage is found via Δ^{-1} , also provided here. Those points with $\Delta_{EW} < 30$ are regarded as low electroweak fine-tuning. Note that the fine-tuning for only the top squarks, represented by $\Delta_{\tilde{t}_{1,2}}$, is of $\mathcal{O}(1)$.

Benchmark	A	B	C	D	E	F	G	H	I
Δ_{EW}	119	62	23	46	45	45	28	40	43
Δ_{EW}^{-1}	0.8%	1.6%	4.4%	2.2%	2.2%	2.2%	3.6%	2.5%	2.3%
$\Delta_{\tilde{t}_1}$	3.4	4.2	3.4	3.9	3.9	3.8	2.9	3.0	3.7
$\Delta_{\tilde{t}_1}^{-1}$	29%	24%	30%	25%	26%	26%	35%	33%	27%
$\Delta_{\tilde{t}_2}$	4.0	5.1	4.0	2.3	2.7	2.8	6.1	5.4	2.8
$\Delta_{\tilde{t}_2}^{-1}$	25%	20%	25%	43%	37%	36%	16%	19%	36%

CONCLUSION

In the search for SUSY, naturalness has been elevated in significance given its prospects for an elegant natural solution to the hierarchy problems and associated low electroweak fine-tuning. In conjunction, the smallness of the higgsinos and light stops required by naturalness introduces an element of uncertainty into observation of natural models at the LHC given the soft nature of the jets. We examined the well-studied GUT model flipped $SU(5)$ with extra vector-like flippon multiplets, known as \mathcal{F} - $SU(5)$. However, in this work we allowed freedom on the No-Scale Supergravity boundary conditions at the unification scale, replicating the flipped $SU(5) \times U(1)_X$ GUT representation, referred to as the D-brane inspired

model (“inspired” due to its forbidden Yukawa coupling terms).

After a rather comprehensive search for a naturalness sector, we uncovered a region highlighted with points exhibiting a low amount of electroweak fine-tuning, namely $\Delta_{EW} < 30$. The naturalness sector was exposed by constraining the model via $M(\tilde{g}) \geq 1.6$ TeV, $124 \leq m_h \leq 128$ GeV, $\Omega h^2 \leq 0.1221$, $\sigma_{SI}^{\text{Rescaled}} \leq 1.5$ pb, and $\Delta M(\tilde{t}_1, \tilde{\chi}_1^0) \leq 5$ GeV, providing us with points possessing $\Delta_{EW} < 30$. Attainment of a light Higgs boson mass consistent with the empirically measured value was strengthened by including contributions from the vector-like flip-pon multiplets, a crucial maneuver given the smallness of the light stops compulsory within naturalness. The resulting region was rather narrow and uniformly supported by nearly 100% branching fractions for the decay channels $\tilde{g} \rightarrow \tilde{t}_1 t$ and $\tilde{t}_1 \rightarrow c\tilde{\chi}_1^0$, indicating the production of a very hard top quark but also a considerably soft charm jet that will be quite difficult to extract from the SM background. Bolstered by these results, we gauged the model against the LHC constraint on $\tilde{t}_1 \rightarrow c\tilde{\chi}_1^0$, finding that indeed our naturalness region uncovered here does skirt just under the ATLAS and CMS exclusion curves on $\tilde{t}_1 \rightarrow c\tilde{\chi}_1^0$.

Could natural SUSY be obscured by the dense Standard Model background in this region heretofore inaccessible at the LHC? Time will tell whether the LHC will yield an affirmative answer to this provocative question. Our imperative here was to merely present a viable physical model that thrives within this elusive space, furnishing motivation to develop enhanced methods of detection for probing concealed SUSY models such as the D-brane inspired model we explored in this work.

ACKNOWLEDGMENTS

Portions of this research were conducted with high performance computational resources provided by the Louisiana Optical Network Infrastructure (<http://www.loni.org>). This research was supported in part by the Projects 11475238, 11647601, and 11875062 supported by the National Natural Science Foundation of China (TL), by the Key Research Program of Frontier Science, Chinese Academy of Sciences (TL), and by the DOE grant DE-FG02-13ER42020 (DVN).

[1] M. Masciovecchio (ATLAS/CMS), “Strong SUSY Results in ATLAS and CMS @ LHC Run II,” (2019), conference: Moriond EW 2019, La Thuile (16-23 March 2019).
 [2] G. Aad et al. (ATLAS), “Observation of a new particle in the search for the Standard Model Higgs boson with the ATLAS detector at the LHC,” Phys. Lett. **B716**, 1 (2012), 1207.7214.

[3] S. Chatrchyan et al. (CMS), “Observation of a new boson at a mass of 125 GeV with the CMS experiment at the LHC,” Phys. Lett. **B716**, 30 (2012), 1207.7235.
 [4] S. M. Barr, “A New Symmetry Breaking Pattern for $SO(10)$ and Proton Decay,” Phys. Lett. **B112**, 219 (1982).
 [5] J. P. Derendinger, J. E. Kim, and D. V. Nanopoulos, “Anti- $SU(5)$,” Phys. Lett. **B139**, 170 (1984).
 [6] I. Antoniadis, J. R. Ellis, J. S. Hagelin, and D. V. Nanopoulos, “Supersymmetric Flipped $SU(5)$ Revitalized,” Phys. Lett. **B194**, 231 (1987).
 [7] I. Antoniadis, J. R. Ellis, J. S. Hagelin, and D. V. Nanopoulos, “An Improved $SU(5) \times U(1)$ Model from Four-Dimensional String,” Phys. Lett. **B208**, 209 (1988), [Addendum: Phys. Lett. **B213**, 562(1988)].
 [8] I. Antoniadis, J. R. Ellis, J. S. Hagelin, and D. V. Nanopoulos, “The Flipped $SU(5) \times U(1)$ String Model Revamped,” Phys. Lett. **B231**, 65 (1989).
 [9] J. L. Lopez, D. V. Nanopoulos, and K.-j. Yuan, “The Search for a realistic flipped $SU(5)$ string model,” Nucl. Phys. **B399**, 654 (1993), hep-th/9203025.
 [10] J. E. Kim and B. Kyae, “Flipped $SU(5)$ from $Z(12-I)$ orbifold with Wilson line,” Nucl. Phys. **B770**, 47 (2007), hep-th/0608086.
 [11] J.-H. Huh, J. E. Kim, and B. Kyae, “ $SU(5)$ (flip) \times $SU(5)$ -prime from $Z(12-I)$,” Phys. Rev. **D80**, 115012 (2009), 0904.1108.
 [12] R. Blumenhagen, S. Moster, and T. Weigand, “Heterotic GUT and standard model vacua from simply connected Calabi-Yau manifolds,” Nucl. Phys. **B751**, 186 (2006), hep-th/0603015.
 [13] C. M. Chen, G. V. Kraniotis, V. E. Mayes, D. V. Nanopoulos, and J. W. Walker, “A Supersymmetric flipped $SU(5)$ intersecting brane world,” Phys. Lett. **B611**, 156 (2005), hep-th/0501182.
 [14] C.-M. Chen, V. E. Mayes, and D. V. Nanopoulos, “Flipped $SU(5)$ from D-branes with type IIB fluxes,” Phys. Lett. **B633**, 618 (2006), hep-th/0511135.
 [15] C.-M. Chen, T. Li, and D. V. Nanopoulos, “Flipped and unflipped $SU(5)$ as type IIA flux vacua,” Nucl. Phys. **B751**, 260 (2006), hep-th/0604107.
 [16] J. Jiang, T. Li, D. V. Nanopoulos, and D. Xie, “F- $SU(5)$,” Phys. Lett. **B677**, 322 (2009), 0811.2807.
 [17] J. Jiang, T. Li, D. V. Nanopoulos, and D. Xie, “Flipped $SU(5) \times U(1)_X$ Models from F-Theory,” Nucl. Phys. **B830**, 195 (2010), 0905.3394.
 [18] J. Jiang, T. Li, and D. V. Nanopoulos, “Testable Flipped $SU(5) \times U(1)_X$ Models,” Nucl. Phys. **B772**, 49 (2007), hep-ph/0610054.
 [19] T. Li, J. A. Maxin, D. V. Nanopoulos, and J. W. Walker, “The Golden Point of No-Scale and No-Parameter $\mathcal{F}-SU(5)$,” Phys. Rev. **D83** (2011).
 [20] T. Li, J. A. Maxin, D. V. Nanopoulos, and J. W. Walker, “The Ultrahigh jet multiplicity signal of stringy no-scale $\mathcal{F}-SU(5)$ at the $\sqrt{s} = 7$ TeV LHC,” Phys. Rev. **D84**, 076003 (2011), 1103.4160.
 [21] T. Li, J. A. Maxin, D. V. Nanopoulos, and J. W. Walker, “A Higgs Mass Shift to 125 GeV and A Multi-Jet Supersymmetry Signal: Miracle of the Flippons at the $\sqrt{s} = 7$ TeV LHC,” Phys. Lett. **B710**, 207 (2012), 1112.3024.
 [22] T. Li, J. A. Maxin, and D. V. Nanopoulos, “The return of the King: No-Scale $\mathcal{F}-SU(5)$,” Phys. Lett. **B764**, 167 (2017), 1609.06294.
 [23] R. De Benedetti, C. Li, T. Li, A. Lux, J. A. Maxin,

- and D. V. Nanopoulos, “Inspiration from intersecting D-branes: general supersymmetry breaking soft terms in no-scale \mathcal{F} -SU(5),” *Eur. Phys. J.* **C78**, 958 (2018), 1809.09695.
- [24] W. Ahmed, L. Calibbi, T. Li, S. Raza, J.-S. Niu, and X.-C. Wang, “Naturalness and Dark Matter in a Realistic Intersecting D6-Brane Model,” *JHEP* **06**, 126 (2018), 1711.10225.
- [25] T. Leggett, T. Li, J. A. Maxin, D. V. Nanopoulos, and J. W. Walker, “Confronting Electroweak Fine-tuning with No-Scale Supergravity,” *Phys.Lett.* **B740**, 66 (2015), 1408.4459.
- [26] J. R. Ellis, K. Enqvist, D. V. Nanopoulos, and F. Zwirner, “Observables in Low-Energy Superstring Models,” *Mod.Phys.Lett.* **A1**, 57 (1986).
- [27] R. Barbieri and G. Giudice, “Upper Bounds on Supersymmetric Particle Masses,” *Nucl.Phys.* **B306**, 63 (1988).
- [28] T. Li, J. A. Maxin, and D. V. Nanopoulos, “Probing the No-Scale \mathcal{F} -SU(5) one-parameter model via gluino searches at the LHC2,” *Phys. Lett.* **B773**, 54 (2017), 1705.07973.
- [29] T. Li, J. A. Maxin, D. V. Nanopoulos, and J. W. Walker, “No-Scale \mathcal{F} -SU(5) in the Light of LHC, Planck and XENON,” *Jour.Phys.* **G40**, 115002 (2013), 1305.1846.
- [30] ATLAS, “Exotics Combined Summary Plots,” (2016), <https://twiki.cern.ch/twiki/bin/view/AtlasPublic/ExoticsPublicResults>.
- [31] R. Harnik, D. T. Larson, H. Murayama, and M. Thormeier, “Probing the Planck scale with proton decay,” *Nucl.Phys.* **B706**, 372 (2005), hep-ph/0404260.
- [32] J. R. Ellis, D. V. Nanopoulos, and K. A. Olive, “Flipped heavy neutrinos: From the solar neutrino problem to baryogenesis,” *Phys.Lett.* **B300**, 121 (1993), hep-ph/9211325.
- [33] J. R. Ellis, J. L. Lopez, D. V. Nanopoulos, and K. A. Olive, “Flipped angles and phases: A Systematic study,” *Phys.Lett.* **B308**, 70 (1993), hep-ph/9303307.
- [34] T. Li, J. A. Maxin, D. V. Nanopoulos, and J. W. Walker, “Dark Matter, Proton Decay and Other Phenomenological Constraints in \mathcal{F} -SU(5),” *Nucl. Phys.* **B848**, 314 (2011), 1003.4186.
- [35] T. A. Aaltonen (Tevatron Electroweak Working Group, CDF, D0), “Combination of CDF and DO results on the mass of the top quark using up to $8.7 fb^{-1}$ at the Tevatron,” (2013), 1305.3929.
- [36] G. Hinshaw et al. (WMAP), “Nine-Year Wilkinson Microwave Anisotropy Probe (WMAP) Observations: Cosmological Parameter Results,” *Astrophys. J. Suppl.* **208**, 19 (2013), 1212.5226.
- [37] N. Aghanim et al. (Planck), “Planck 2018 results. VI. Cosmological parameters,” (2018), 1807.06209.
- [38] Y. Huo, T. Li, D. V. Nanopoulos, and C. Tong, “The Lightest CP-Even Higgs Boson Mass in the Testable Flipped $SU(5) \times U(1)_X$ Models from F-Theory,” *Phys.Rev.* **D85**, 116002 (2012), 1109.2329.
- [39] M. Aaboud et al. (ATLAS), “Search for dark matter and other new phenomena in events with an energetic jet and large missing transverse momentum using the ATLAS detector,” *JHEP* **01**, 126 (2018), 1711.03301.
- [40] M. Aaboud et al. (ATLAS), “Search for supersymmetry in final states with charm jets and missing transverse momentum in 13 TeV pp collisions with the ATLAS detector,” (2018), 1805.01649.
- [41] HFAG (2013), www.slac.stanford.edu/xorg/hfag/rare/2013/radll/OUTPUT/TABLES/radll.pdf.
- [42] V. Khachatryan et al. (LHCb, CMS), “Observation of the rare $B_s^0 \rightarrow \mu^+ \mu^-$ decay from the combined analysis of CMS and LHCb data,” *Nature* **522**, 68 (2015), 1411.4413.
- [43] T. Aoyama, M. Hayakawa, T. Kinoshita, and M. Nio, “Complete Tenth-Order QED Contribution to the Muon $g-2$,” *Phys.Rev.Lett.* **109**, 111808 (2012), 1205.5370.
- [44] D. S. Akerib et al., “Results from a search for dark matter in LUX with 332 live days of exposure,” (2016), 1608.07648.
- [45] A. Tan et al. (PandaX-II), “Dark Matter Results from First 98.7-day Data of PandaX-II Experiment,” *Phys. Rev. Lett.* **117**, 121303 (2016), 1607.07400.
- [46] E. Aprile et al. (XENON), “Dark Matter Search Results from a One Tonne \times Year Exposure of XENON1T,” (2018), 1805.12562.
- [47] G. Belanger, F. Boudjema, A. Pukhov, and A. Semenov, “Dark matter direct detection rate in a generic model with micrOMEGAs2.1,” *Comput. Phys. Commun.* **180**, 747 (2009), 0803.2360.
- [48] A. Djouadi, J.-L. Kneur, and G. Moultaka, “SuSpect: A Fortran code for the supersymmetric and Higgs particle spectrum in the MSSM,” *Comput. Phys. Commun.* **176**, 426 (2007), hep-ph/0211331.
- [49] A. Djouadi, M. M. Muhlleitner, and M. Spira, “Decays of supersymmetric particles: The Program SUSY-HIT (SuSpect-SdecaY-Hdecay-InTerface),” *Acta Phys. Polon.* **B38**, 635 (2007), hep-ph/0609292.
- [50] M. Tanabashi et al. (Particle Data Group), “Review of Particle Physics,” *Phys. Rev.* **D98**, 030001 (2018).
- [51] A. M. Sirunyan et al. (CMS), “Search for new phenomena with the M_{T2} variable in the all-hadronic final state produced in proton-proton collisions at $\sqrt{s} = 13$ TeV,” *Eur. Phys. J.* **C77**, 710 (2017), 1705.04650.
- [52] A. M. Sirunyan et al. (CMS), “Search for direct production of supersymmetric partners of the top quark in the all-jets final state in proton-proton collisions at $\sqrt{s} = 13$ TeV,” *JHEP* **10**, 005 (2017), 1707.03316.
- [53] A. M. Sirunyan et al. (CMS), “Search for natural and split supersymmetry in proton-proton collisions at $\sqrt{s} = 13$ TeV in final states with jets and missing transverse momentum,” *JHEP* **05**, 025 (2018), 1802.02110.
- [54] A. M. Sirunyan et al. (CMS), “Search for the pair production of third-generation squarks with two-body decays to a bottom or charm quark and a neutralino in proton-proton collisions at $\sqrt{s} = 13$ TeV,” *Phys. Lett.* **B778**, 263 (2018), 1707.07274.
- [55] H. Baer, V. Barger, P. Huang, A. Mustafayev, and X. Tata, “Radiative natural SUSY with a 125 GeV Higgs boson,” *Phys. Rev. Lett.* **109**, 161802 (2012), 1207.3343.
- [56] H. Baer, V. Barger, P. Huang, D. Mickelson, A. Mustafayev, and X. Tata, “Post-LHC7 fine-tuning in the minimal supergravity/CMSSM model with a 125 GeV Higgs boson,” *Phys. Rev.* **D87**, 035017 (2013), 1210.3019.